Arabian Journal of Geosciences (2020) 13: 1163
https://doi.org/10.1007/s12517-020-06191-z

ORIGINAL PAPER

Effect of W-OH, a hydrophilic polyurethane polymer, in controlling erosion of two typical erodible soils in southern China

Xuchao Zhu[1] · Yin Liang[1] · Zhiyuan Tian[1] · Xin Wang[1,2] · Xinzhen Qiu[3]

Received: 5 June 2020 / Accepted: 27 October 2020 / Published online: 31 October 2020

Abstract

A new hydrophilic polyurethane polymer, W-OH, has recently been widely used in southern China to control soil erosion, but the theory of its effectiveness lags behind the practice. We used two typically erodible soils, red clay soil (RCS) from sloping farmland and *benggang* sandy soil (BSS) from collapsing gullies, in southern China as test objects to analyze the effect of spraying W-OH on the characteristics of soil aggregates, infiltration, runoff, and sediment transport in indoor controlled experiments and outdoor simulated rainfall experiments. The mean diameter of the aggregate increased, the fractal dimension decreased, and the water-stable aggregate content increased in RCS and BSS as the concentration of W-OH increased from 0 to 7%. Spraying 5% W-OH significantly decreased the infiltration rate for both soils. Spraying W-OH increased the mean RCS and BSS runoff rates by 190 and 37.3% but decreased the sediment yields by 74.1 and 62.1%, respectively, and showed a good soil erosion control effect. Spraying W-OH also affected the leaching of nutrients, increasing total organic carbon content by 170 and 330% for RCS and BSS, respectively. This study provides theoretical supplementation for the application of W-OH for controlling soil erosion from sloping farmland and *benggangs* in southern China.

Keywords Hydrophilic polyurethane polymer · Soil aggregate · Soil erosion · Red soil region · *Benggang* · Simulated rainfall

Introduction

Soil erosion occurs widely around the world and is an important manifestation of soil degradation (Lal 2003). The area in China where soil and water have been lost was 2.737 million km^2 by 2018, and southern China is the main region of erosion caused by water (MWR 2018). Sloping farmland and *benggang*, a landform also known as collapsing gullies where soil erosion is serious, are the main places of soil erosion in southern China. China has about 0.24 million km^2 of sloping farmland, most of which is distributed in the southern erosion area where 1.415×10^9 t/year is eroded, accounting for 31% of the total amount of soil erosion in China (MWR et al. 2010). *Benggangs* are mainly distributed in the southern red soil region, which contains about 2.4×10^5 *benggangs*, although the total area of erosion is not large; average erosion is as high as 5.9×10^4 t/(km^2 year), which is a large problem (Liang et al. 2009; MWR et al. 2010). Serious soil erosion in sloping farmland and *benggangs* degrades the land, reduces agricultural production, pollutes the environment, and causes other problems that threaten the survival and development of local populations (Baskan et al. 2010; Liang et al. 2010).

The problem of the erosion of red clay soil (RCS) from sloping farmland and *benggang* sandy soil (BSS) from collapsing gullies in southern China has been widely studied. Studies have mainly focused on the intensity (Liang et al. 2009), processes (Wang et al. 2016; Jiang et al. 2018), mechanism (Lin et al. 2015; Jiang et al. 2018), and control measures (De Baets et al. 2009; Muukkonen et al. 2009; Zhong et al. 2013) of soil erosion, which have provided a solid theoretical foundation for preventing and controlling the erosion of these two typical soils. The control measures have mainly included biological (Zhong et al. 2013; Cao et al. 2015b);

Responsible Editor: Amjad Kallel

✉ Yin Liang
yliang@issas.ac.cn

[1] State Key Laboratory of Soil and Sustainable Agriculture, Institute of Soil Science, Chinese Academy of Sciences, Nanjing 210008, China

[2] College of Resources and Environment, University of Chinese Academy of Sciences, Beijing 100190, China

[3] Soil and Water Conservation Bureau of Ganxian District, Ganxian, Ganzhou 341100, China

comprehensive biological and engineering (Zhong et al. 2013); and biological, engineering, and chemical (Zhang et al. 2014; Zhu et al. 2017; Sun and Zhang 2018) measures, all of which have been effective. Comprehensive control measures that include chemical materials can prevent the secondary erosion of soil where the vegetation was not restored after engineering measures, which control erosion well and have recently been widely used (Zhang et al. 2014; Liang et al. 2017; Zhu et al. 2017; Tang and She 2018).

W-OH is a hydrophilic polyurethane polymer that uses water as a reactant. W-OH can be rapidly cemented by water to form an elastic porous layer in the topsoil, which can substantially reduce the intensity of soil erosion (Zhu et al. 2017). W-OH has the advantages over traditional chemical soil amendments (such as PAM and EN-1) of stability, modifiability, and environmental friendliness (Yao et al. 2015), so W-OH has been widely and successfully used in the field for conserving soil and water, especially in the restoration and control of *benggangs* and the prevention and control of soil erosion on sloping farmland in southern China (Zhu et al. 2017; Liang et al. 2017, 2019). The theoretical bases of the effects of W-OH application on controlling soil erosion, however, remain incompletely studied. For example, the effects of W-OH on soil aggregates and soil-water content (SWC) are not clear, and the characteristics of infiltration, erosion, and associated nutrient processes after spraying W-OH are also not clear. Our theoretical understanding thus lags behind practice, which limits the further application of W-OH for controlling soil erosion in southern China. The characteristics of soil aggregates, infiltration rate, runoff, and sediment and associated nutrient processes of the soils before and after spraying W-OH should be determined and analyzed to provide a theoretical basis for the application of W-OH to control soil erosion.

The specific objectives of this study were therefore to (a) identify the effect of W-OH on soil properties associated with erosion, e.g., soil aggregates and SWC, (b) understand the characteristics of water infiltration in RCS and BSS under various concentrations of W-OH, and (c) clarify the processes of runoff, sediment, and associated nutrient transport for the two soils under the influence of W-OH.

Materials and methods

Study site

This study was carried out at the Ecological Experimental Station of Red Soil of the Chinese Academy of Sciences, in Yingtan City, Jiangxi Province, China (28°12′19″N, 116°55′31″E; Fig. 1). The experimental RCS was obtained from local typical sloping farmland. This area has a subtropical monsoon climate with a mean annual temperature of 17.8 °C and mean annual rainfall of about 1800 mm, which falls mainly from April to June (Gao et al. 2019). The terrain is mainly low hills and gentle slopes with gradients of 3–15°. The soil parental material is quaternary RCS and red sandstone, and the soil is a typical RCS with a heavy texture, poor aeration and permeability, and high acidity (Gao et al. 2020).

BSS was obtained from Ganzhou City, Jiangxi Province, China (26°11′58″N, 115°11′15″E; Fig. 1), which has a humid moderate subtropical monsoon climate with a mean annual temperature of 19.3 °C and mean annual rainfall of 1076 mm, distributed unevenly throughout the year but with 47.5% falling from April to June. The terrain in this area is mainly hilly land with steep slopes at an altitude of 500–1000 m. Red-brown soil developed from granite is distributed widely and contains a large amount of quartz sand and gravel. The soil texture is relatively rough, which leads to serious leaching of water and fertilizer. The occurrence and development of *benggangs* are typical in this area (Deng et al. 2019).

The names RCS and BSS in this study are a combination of Chinese soil taxonomic name and the local names and correspond to clay loam and sandy clay loam, respectively, in the commonly used standard classification of soil texture by the United States Department of Agriculture, with sand, silt, and clay contents of 32.28, 33.2, and 34.54% and 62.15, 29.91, and 7.93%, respectively. Other basic physical and chemical properties of the two soils are presented in Table 1.

Experimental design

Aggregate experiment

Soil erosion is closely associated with the aggregate of the soil, so determining and analyzing the characteristics of aggregates for RCS and BSS under different W-OH conditions are important for understanding the anti-erosion mechanism of W-OH. We used 400-cm^3 cutting rings (5 cm in radius and height) to obtain undisturbed samples of the two soils at their typical sites; sprayed the samples with W-OH (20 ml for each sample) at concentrations of 0, 1, 3, and 5% in the laboratory; and then put the samples in an outdoor natural environment. We used dry and wet sieving to determine the quantity and distribution of the aggregates of the two soils 1, 2, and 3 months after spraying, with two replicates for each soil type and W-OH concentration. Mean weight diameter (MWD), geometric mean diameter (GMD), fractal dimension (D), and water-stable aggregate (WSA, > 0.25 mm) contents were used to describe the characteristics of the aggregates (Qi et al. 2018; Jia et al. 2019; Ye et al. 2019).

Infiltration experiment

Cutting rings were used for determining the characteristics of infiltration for RCS and BSS under different W-OH

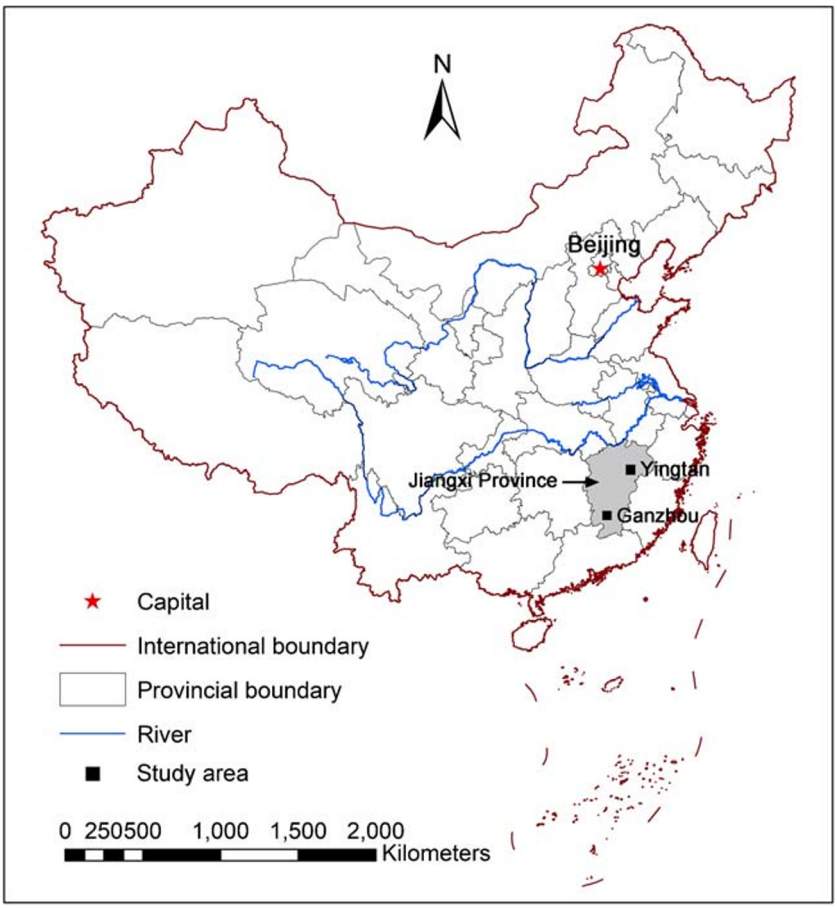

Fig. 1 Location of the study areas

concentrations. The samples of the two soils were air-dried and passed through a 2-mm sieve into 400-cm^3 cutting rings at bulk densities similar to the natural soils. W-OH at concentrations of 0, 1, 3, 5, and 7% were sprayed onto the surface of the soils in the cutting rings, with two replicates for each soil type and concentration. Empty cutting rings were placed on the cutting rings containing the soil samples, and the interfaces were sealed with plastic encapsulating bands and adhesive tape. Filter paper was placed at the bottom of the empty cutting rings to eliminate the potential erosion from pouring water on the surface of the soils. Fifty milliliters of distilled water was then slowly poured into the upper cutting ring, and the time when the water completely disappeared on the filter paper was recorded. Another 50 ml of distilled water was then poured into the ring, and the time when the water completely disappeared was again recorded. This process was repeated until the time needed for the water to disappear stabilized. The rates and processes of infiltration for the two soils at the various W-OH concentrations could thus be deduced and analyzed.

Simulated rainfall experiment

The dynamics of runoff and sediment transport for RCS and BSS with and without W-OH were experimentally determined using simulated rainfall. This experiment consisted of the two soil types, RCS and BSS, and two W-OH concentrations, 0 and 5%. The simulated rainfall experiment was conducted in runoff microplots made from stainless-steel plates 2, 1, and 0.6 m in length, width, and height, respectively. The slope

Table 1 Basic soil properties of the red clay soil (RCS) and the *benggang* sandy soil (BSS)

Soil type	BD (g/cm^3)	CP (%)	pH	SOM (g/kg)	TN (g/kg)	TP (g/kg)	TK (g/kg)	Sand (%)	Silt (%)	Clay (%)
RCS	1.63	27.61	4.49	6.71	0.46	0.25	11.43	32.28	33.20	34.52
BSS	1.36	44.59	5.38	2.23	0.04	0.16	10.59	62.15	29.91	7.93

BD, soil bulk density; *CP*, capillary porosity; *SOM*, soil organic matter content; *TN*, total nitrogen content; *TP*, total phosphorus content; *TK*, total potassium content; *San*d, sand (0.05–2 mm) content; *Silt*, silt (0.002–0.05 mm) content; *Clay*, clay (< 0.002 mm) content. The percentages of sand, silt, and clay content were determined using the standard sieve-pipette method

could be adjusted from 0 to 40°, and holes were evenly drilled in the bottom plates of the plots to facilitate the drainage. A V-shaped spout was installed at the base of the slope to collect samples of runoff and sediment. The soil slope was set at 15°, a common average slope where RCS and BSS were collected. The soils in the plots were air-dried and large clods were broken, and the soils were then passed through a 10-cm sieve before adding to the plots. The simulated rainfall experiment was carried out after the soil was allowed to settle naturally for about 1 month.

A portable artificial rainfall simulator was used, mainly consisting of a nozzle, support frame, water pump, and pressure gauge. The support frame was composed of four 3-m steel pipes. The nozzle was about 3 m above the surface of the soil and produced rainfall at an intensity of 80 mm/h. The terminal velocity and energy of the raindrops were similar to those of natural rainfall (Meyer and Harmon 1979; Cao et al. 2015a). A uniformity coefficient for each rainfall was calculated using four gauges at the corners of each plot before the rainfall began. The direction and height of the nozzle were adjusted to ensure the uniformity coefficient was > 80%. Samples of runoff and sediment were collected in 500-ml bottles every 3 min after runoff first appeared, and the sampling time was recorded for each bottle. Each rainfall lasted for about 1 h, so 20 samples of runoff and sediment were collected during each rainfall. The runoff volume was measured, and the sediment was weighed, in the laboratory (Tian et al. 2017). The contents of total organic carbon (TOC), total nitrogen (TN), ammonium nitrogen (AN), nitrate nitrogen (NN), and total potassium (TK) in the runoff samples were measured using a carbon and nitrogen analyzer by colorimetry and flame photometry, respectively. Four consecutive runoff samples were combined into one sample for testing and determining the nutrient contents to reduce sampling errors and costs. Five water samples in addition to the background rainwater sample were sent to the analysis and test center of the Institute of Soil Science for determining the TOC, TN, AN, NN, and TK contents for each simulated rainfall.

Measurement of SWC

This experiment was conducted to compare changes in SWC for RCS and BSS before and after the simulated rainfall at 0 and 5% W-OH. A 75-cm time domain reflectometry (TDR) measuring tube was inserted 50 cm into the middle of each plot and 25 cm above the soil. Trime TDR was used to measure SWC at depths of 10, 20, 30, and 40 cm in each plot before, immediately after, and 24 h after the simulated rainfall. The data were used to characterize the response of SWC to the rainfall at 0 and 5% W-OH.

Statistics and analysis

Basic data analyses and calculations in this study were conducted using Microsoft Excel 2016. Variables and indices (i.e., infiltration rate, runoff rate, sediment yield, SWC, and the aggregate indices) for the two soils at the various W-OH concentrations were analyzed using SPSS 20. A one-way analysis of variance (ANOVA) was used to test the significance of differences between variable means. Figures were drawn using Origin 2017.

Results and discussion

Effect of W-OH concentration on soil aggregates

MWD and GMD are common indices of the size and distribution of soil aggregates, and the larger their values, the higher the aggregation and aggregate stability (Nimmo and Perkins 2002). Both MWD and GMD for dry RCS and BSS aggregates increased with W-OH concentration (Fig. 2a, c). MWD increased by 9.6 and 17.2% and GMD increased by 11.9 and 25.2% for RCS and BSS, respectively, as the W-OH concentration increased from 0 to 7%. The increases for wet MWD and GMD aggregates were small (Fig. 2b, d); MWD for RCS and BSS increased by 6.0 and 3.2%, respectively, and GMD for BSS increased by 3.3%. These results indicated that W-OH could improve aggregation and aggregate stability and thus decrease the erodibility of the two soils. The effect of W-OH on aggregation was better for BSS than for RCS, because BSS was coarser, allowing the W-OH solution to infiltrate deeper before it coagulated and could thus bind more soil particles (Fig. 2).

D is an important index for describing the distribution of aggregates; the smaller the D is, the more stable the soil structure (Jia et al. 2019). D for both dry and wet aggregates of the two soils decreased as the W-OH concentration increased (Fig. 2e, f), and the decrease was larger for BSS than for RCS. These results indicated that W-OH could facilitate the aggregation of soil particles and stabilize the soil structure and that BSS responded better than RCS.

WSA content is an index that is directly correlated with soil erosion; the larger the content, the lower the erodibility of the soil (Ye et al. 2019). WSA content for RCS ranged from 27.5 to 32.6% and increased by 18.5% as the W-OH concentration increased. WSA content for BSS ranged from 53.9 to 64.1% and increased by 18.9% as the W-OH concentration increased (Fig. 2g). These results indicated that W-OH could increase WSA content for both soils and thus decrease their erodibility. WSA content was notably about twofold higher for BSS than for RCS, which was unexpected and inconsistent with the results of similar studies (Wang et al. 2016; Lin et al. 2018). This abnormal result was likely due to the high contents of

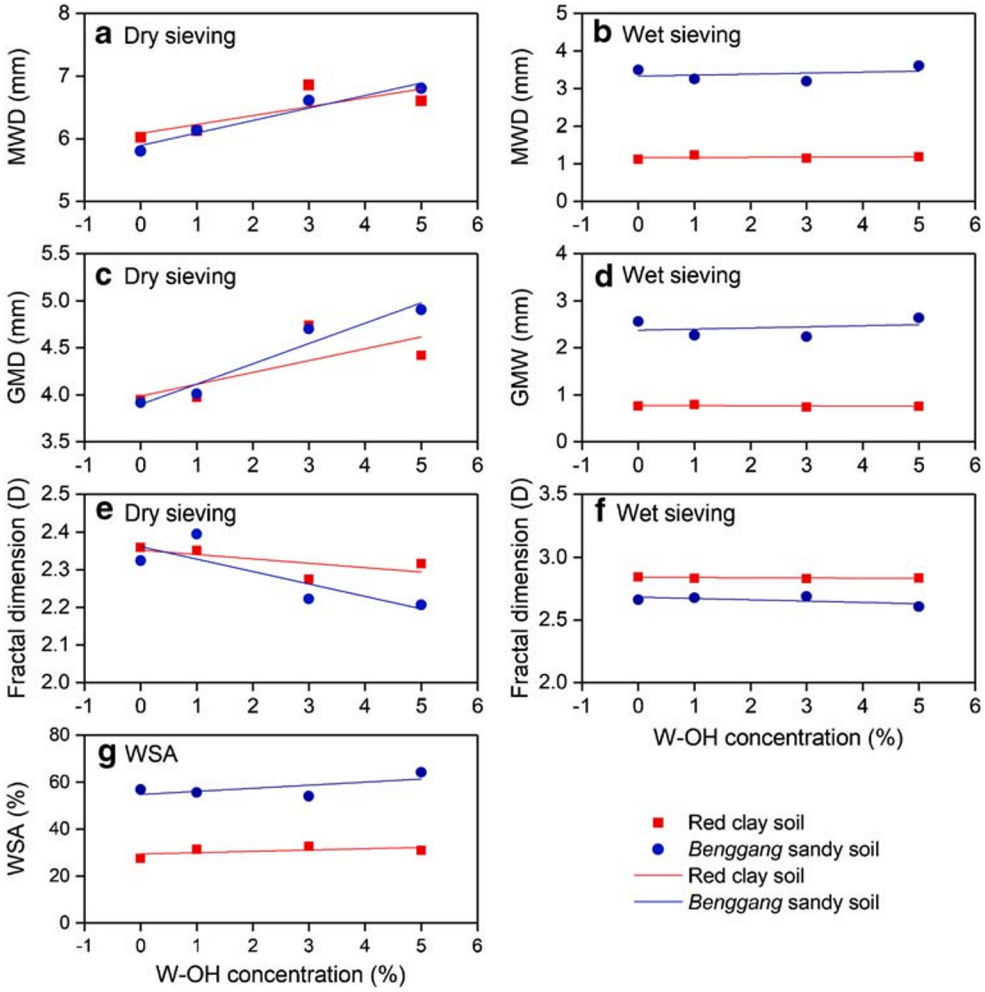

Fig. 2 Effects of W-OH concentration (0, 1, 3 and 5%) on dry-sieved soil mean weight diameter (MWD, **a**), dry-sieved geometric mean diameter (GMD, **c**), dry-sieved fractal dimension (D, **e**), wet-sieved MWD (**b**), wet-sieved GMD (**d**), wet-sieved D (**f**) and water-stable aggregate (WSA, > 0.25 mm, **g**)

sand and quartz particles in BSS, which led to its high WSA content. The textures of the BSS samples we used were nevertheless uniform, so the data could be used for a horizontal comparative analysis of WSA content under the various W-OH concentrations.

The above analysis of the aggregate indices for the two soils at the various W-OH concentrations suggests that spraying W-OH onto the soil surface can increase aggregation and the stability of the aggregates and thereby decrease soil erodibility. W-OH thus prevented and controlled the erosion of the two soils to some extent.

Characteristics of infiltration at the various W-OH concentrations

The rates of infiltration of rainwater into RCS and BSS at the various W-OH concentrations are shown in Fig. 3. The rates of infiltration for samples sprayed with 0% W-OH tended to first rapidly decline and then stabilize, but the rates for samples sprayed with W-OH tended to first slowly increase and then stabilize at the various W-OH concentrations. These results were likely mainly due to the consolidation of porous colloids that formed on the soil surface after the W-OH was sprayed. The rainwater would have wetted, infiltrated, and permeated the porous colloids (Liang et al. 2016), which would be slower than on a bare soil surface. The infiltration rate slowly increased after water penetrated the colloids and then remained stable when the entire soil sample became saturated. The infiltration rates for the two soils were both significantly higher without than with W-OH, and the rates with W-OH generally decreased as the W-OH concentration increased.

We divided infiltration into initial, mean, and stable infiltration to further analyze its characteristics for the two soils at the various W-OH concentrations (Table 2). The initial and stable rates of infiltration for both soils generally decreased as the W-OH concentration increased. The initial rate decreased from 9.45 to 1.64 mm/min and from 9.59 to 0.97 mm/min for RCS and BSS, respectively, both with similar ranges. The stable rate decreased from 4.79 to 0.61 mm/min and from 3.17 to 2.11 mm/min for RCS and BSS, respectively, and the range was 3.9-fold larger for RCS than for BSS, indicating that the stable rate was more sensitive for RCS than for BSS, likely mainly due to the different particle compositions and

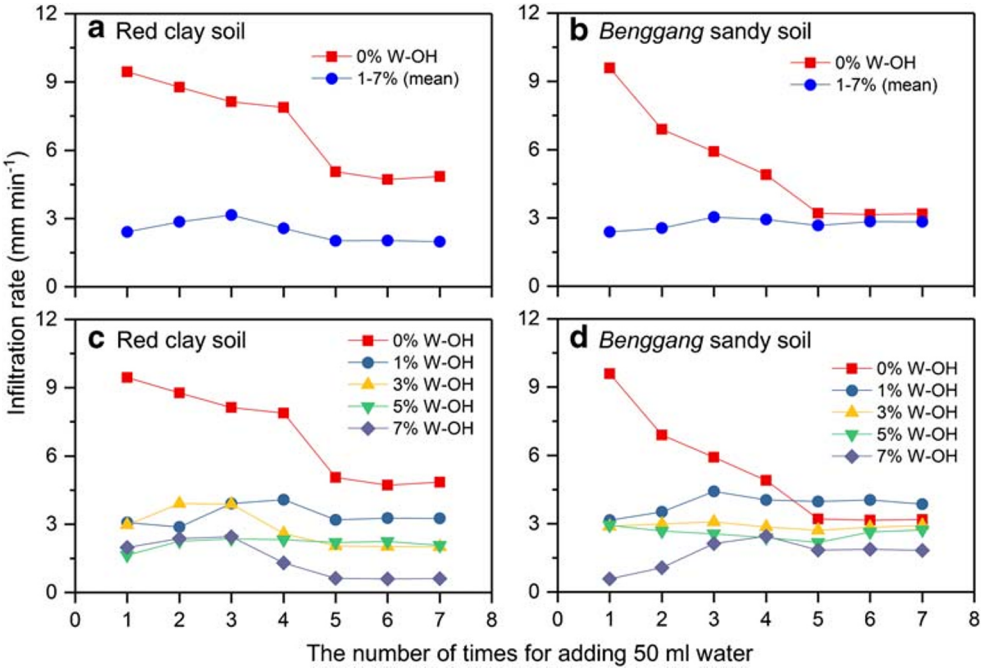

Fig. 3 Infiltration rates for red clay soil (**a**, **c**) and *benggang* sandy soil (**b**, **d**) at the various W-OH concentrations

structures of the two soils. The mean rates at the various W-OH concentrations differed significantly between the soils, indicating that the W-OH concentration strongly affected the mean rates for RCS and BSS. The mean rates at the various W-OH concentrations ranged from 1.42 to 6.98 and from 2.58 to 5.26 mm/min for RCS and BSS, respectively, and the range was 2.1-fold larger for RCS than for BSS, similar to the results for the stable rate and consistent with the characteristics of late infiltration, with some dispersion for RCS and more concentrated for BSS (Fig. 3). These results indicated that W-OH could relatively continuously decrease infiltration for RCS but that the decrease was smaller for BSS. These trends are important for the practical prevention and control of soil erosion using W-OH in southern China.

Effect of W-OH concentration on runoff and sediment transport

We did not carry out a simulated rainfall experiment for each W-OH concentration (i.e., 1, 3, 5, and 7%) due to the number of runoff microplots and the large volume of soil that needed to be transported. We chose the best concentration of 5% after evaluating the actual effect and cost. Runoff and sediment transport for RCS and BSS at W-OH concentrations of 0 and 5% are shown in Fig. 3. The runoff first increased and then fluctuated stably (Fig. 4a, c), because the soil was initially relatively dry and its surface was not covered by water. Erosion from splashes played an important role, so the rate of infiltration was high and the rate of runoff was relatively low. The soil surface became covered by a layer of rainwater

Table 2 Characteristics of infiltration for red clay soil (RCS) and *benggang* sandy soil (BSS) at the various W-OH concentrations

Soil type	W-OH concentration (%)	Initial infiltration rate (mm/min)	Mean infiltration rate (mm/min)	Stable infiltration rate (mm/min)
RCS	0	9.45	6.98A	4.79
	1	3.07	3.38B	3.27
	3	2.97	2.77C	2.01
	5	1.64	2.15D	2.16
	7	1.98	1.42E	0.61
BSS	0	9.58	5.26a	3.17
	1	3.15	3.85b	3.94
	3	2.89	2.89c	2.88
	5	2.93	2.58d	2.68
	7	0.97	2.01e	2.11

Different letters indicate significant differences between mean infiltration rates at $p < 0.01$ (one-way ANOVA)

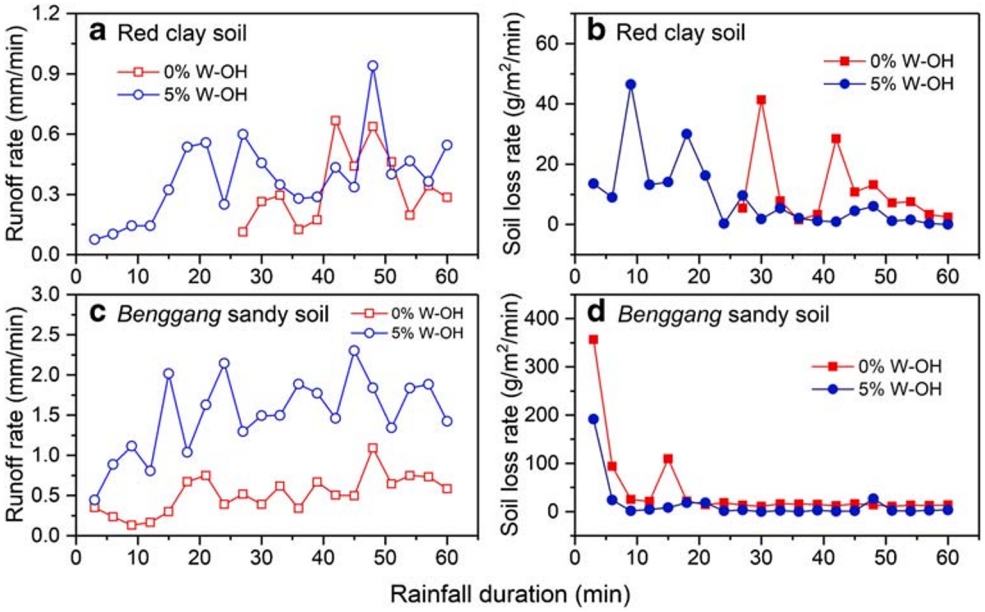

Fig. 4 Variations of the rates of runoff (**a**, **c**) and soil loss (**b**, **d**) at 0 and 5% W-OH concentrations for red clay soil (**a**, **b**) and *benggang* sandy soil (**c**, **d**) during the simulated rainfall

as the rainfall proceeded, the infiltration rate decreased, and surface flow was generated, so runoff increased, consistent with most similar studies (Shen et al. 2016; Jiang et al. 2018; Li et al. 2019). The runoff rate was higher on the BSS slope sprayed with 5% W-OH than on the slope with 0% W-OH (Fig. 4c), and the mean runoff rate increased from 17.19 to 50.17 ml/s. Runoff was not measured for RCS because the samples were damaged earlier during the simulated rainfall. The mean runoff rate for RCS in the stage when we obtained runoff data for the slope with 5% W-OH (15.15 ml/s), however, was significantly higher than the mean runoff rate (11.11 ml/s) at the corresponding stage for the slope with 0% W-OH (ANOVA, $p < 0.01$), and the mean runoff rate increased by 37.3% after spraying with 5% W-OH (Fig. 4a). This result may have been due to the properties of the colloids formed by W-OH, which had a similar effect as the layer of rainwater on the soil surface and could reduce the erosion from splashes and decrease water infiltration (Fig. 3), thereby increasing runoff.

The sediment yield for RCS and BSS in the simulated rainfall first quickly decreased and then fluctuated stably (Fig. 4b, d), because soil particles were loosened by the impact of the raindrops during the stage of splash erosion and then transported in the runoff. Splash erosion decreased as the rainfall continued, and the number of loose and erodible particles on the soil surface decreased, which decreased the rate of soil loss (Jiang et al. 2018). The rates of sediment transport were higher for the slopes sprayed with 0% W-OH than for the slopes with 5% W-OH for both soils, mainly due to the protective effect of W-OH on the particles on the soil surface. The W-OH solution would adhere to the soil particles and form a soil-colloid concretion layer, decreasing the loss of soil particles, consolidating the soil and consequently decreasing erosion (Zhu et al. 2017). Soil loss for RCS was 798.3 g on the slope with 0% W-OH and 207 g for the slope sprayed with 5% W-OH in the rainfall stage, which was only 25.9% of soil loss on the slope without W-OH protection. Total soil loss for BSS throughout the simulated rainfall was 4935.6 g for the slope sprayed with 0% W-OH and 1872 g for the slope sprayed with 5% W-OH, accounting for only 37.9% of the loss for the slope with 0% W-OH.

These results indicated that W-OH had notable effects on the soil and water. The runoff rate increased, and the rate of soil loss decreased, significantly after spraying 5% W-OH on the slopes for both soils. Specifically, the mean runoff rates increased by 190 and 37.3%, and the rate of soil loss decreased by 74.1 and 62.1%, for RCS and BSS, respectively, indicating that W-OH could effectively control soil erosion for these two typical erodible soils in southern China.

Nutrient contents in runoff

We determined the contents of TOC, TN, AN, NN, and TK in the runoff samples and rainwater to understand the effect of W-OH on nutrients in the runoff (Fig. 5). TOC contents in the runoff for the RCS and BSS slopes sprayed with W-OH were significantly higher than the TOC content of the rainwater. The mean TOC contents of the runoffs from the RCS and BSS slopes sprayed with W-OH were 1.7- and 3.3-fold higher, respectively, than the TOC content of the rainwater (Fig. 5a). TOC contents in the runoff for the two soils sprayed with W-OH were also significantly higher than the TOC content without W-OH. Mean TOC content in the runoff from the RCS and BSS slopes was 3.4- and 2.3-fold higher, respectively, with than without W-OH. These results were mainly because W-OH is a macromolecular organic compound, and

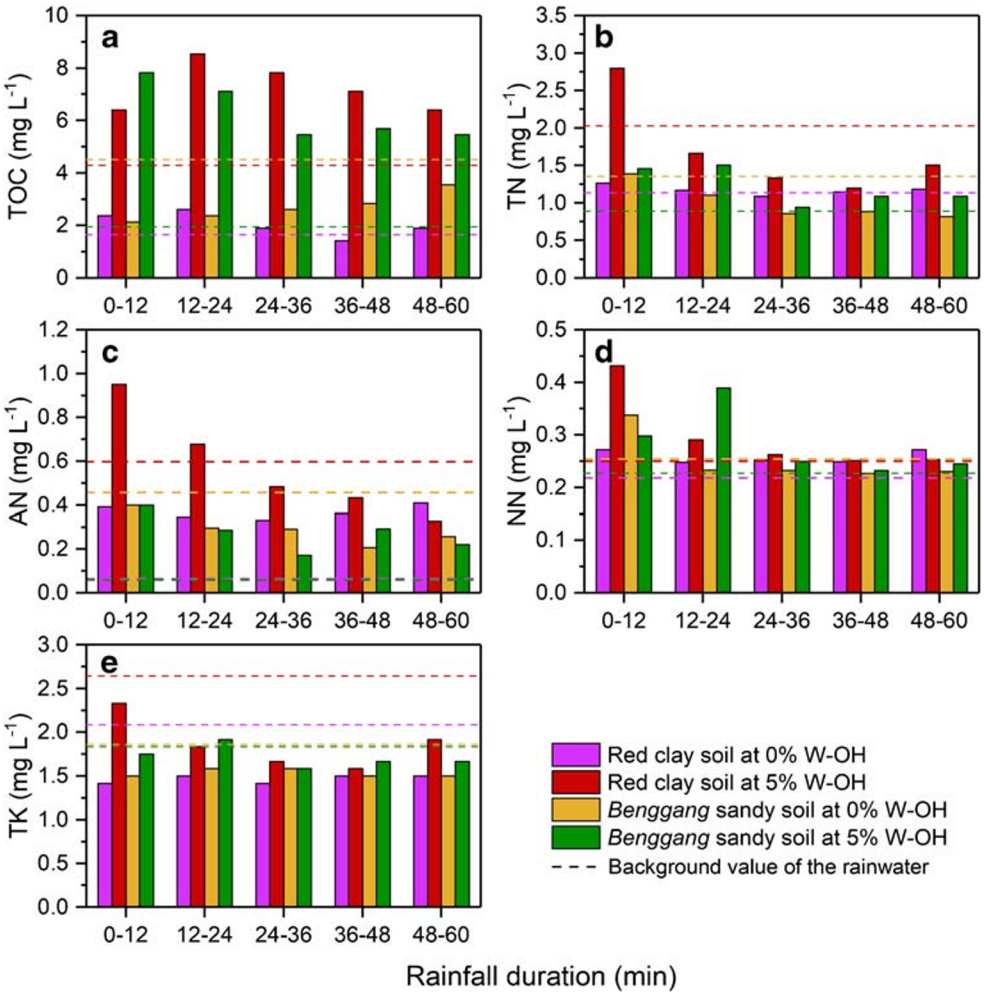

Fig. 5 Contents of **a** total organic carbon (TOC), **b** total nitrogen (TN), **c** ammonium nitrogen (AN), **d** nitrate nitrogen (NN), and **e** total potassium (TK) for runoffs at 0 and 5% W-OH for red clay soil and *benggang* sandy soil

some fine consolidated colloids may be washed away by the runoff during simulated rainfall, leading to a higher TOC content for the runoff than for the rainwater. The TOC content of the runoff decreased on slopes sprayed with W-OH when the rainfall continued, perhaps due to the reduction in fine consolidated colloids on the slopes. The nitrogen content was generally higher for the runoff from the slopes sprayed with W-OH than for both the runoff from slopes without W-OH and the rainwater at the early stage of the simulated rainfall and was similar to the nitrogen content of the runoff without W-OH and the rainwater at the later stages (Fig. 5b–d). This result indicated that spraying with W-OH would initially increase the nitrogen content of the runoff to some extent and then decrease the content to a normal level. W-OH did not increase the TK content of the runoffs from the two soil slopes (Fig. 5e), indicating that using W-OH to control soil erosion did not affect the TK content of the runoff. The above results indicated that spraying with W-OH increased the amount of TOC in the runoff from both the RCS and BSS slopes, had little effect on the nitrogen content, and had no effect on the TK content.

SWC profiles

The distributions of SWC in the RCS and BSS profiles before and after the simulated rainfall at W-OH concentrations of 0 and 5% are shown in Fig. 6. The vertical SWC distributions differed between RCS and BSS, with SWC first decreasing and then increasing for RCS but continuously increasing for BSS before the rainfall (Fig. 6). This difference was mainly due to the higher clay and aggregate contents for RCS than for BSS and led to a higher water-holding capacity for RCS than for BSS. SWC at the various soil depths generally increased to some extent after the rainfall and then decreased by 24 h after the rainfall. Mean SWCs in the runoff microplots with RCS at 0% W-OH, RCS at 5% W-OH, BSS at 0% W-OH, and BSS at 5% W-OH increased by 5.0, 3.7, 1.7, and 2.5%, respectively, after the simulated rainfall relative to the mean SWCs in the plots before the rainfall, and the amount of increase was larger for RCS than for BSS. The mean SWCs of the plots 24 h after the rainfall were still slightly higher than the mean SWCs before the rainfall, which increased by 2.3, 1.7, 1.3, and 1.4%, respectively.

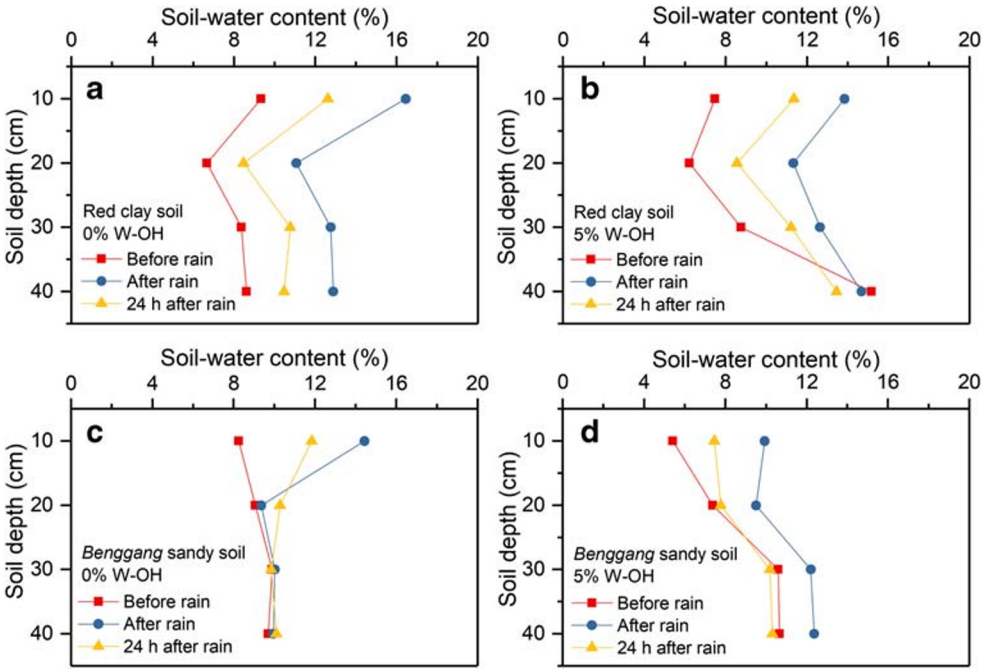

Fig. 6 Profiles of soil-water content at depths of 10, 20, 30, and 40 cm before, immediately after, and 24 h after the simulated rainfall for **a** red clay soil at 0% W-OH, **b** red clay soil at 5% W-OH, **c** *benggang* sandy soil at 0% W-OH, and **d** *benggang* sandy soil at 5% W-OH

The mean SWCs for the two soils before, immediately after, and 24 h after the simulated rainfall at W-OH concentrations of 0 and 5% are presented in Table 3. The mean SWCs for both soils at the three measuring occasions did not all vary consistently at either the 0% or the 5% W-OH concentration. Mean SWC for RCS with 0% W-OH before the rainfall was lower than the mean SWC when sprayed with 5% W-OH, and the mean SWC for BSS with 0% W-OH before the rainfall was higher than the mean SWC when sprayed with 5% W-OH. Mean SWC for RCS was higher with 0 than with 5% W-OH after the simulated rainfall, and mean SWC for BSS was lower with 0 than with 5% W-OH. Mean SWC 24 h after the rainfall was lower with 0 than with 5% W-OH for RCS but was higher for BSS. Mean SWC did not differ significantly between 0 and 5% W-OH (ANOVA, $p > 0.05$), indicating that W-OH had little influence on the mean SWC for both RCS and BSS under these experimental conditions. This result may have been due to two factors: (1) the thickness of the soil in the microplots was only 50 cm, which did not accurately represent the distribution of SWC in the profiles of the two soils, and (2) the experimental microplots were about 30 cm above the ground and their soils were not in contact with the ground, so the soils were more prone to leaching water than was the soil in the runoff plot on the ground, leading to a drier soil. W-OH can increase runoff, reduce water infiltration and evaporation from soil, and theoretically should also affect SWC. The effect of W-OH on SWC therefore needs further study with conditions more similar to natural conditions, which is also important for alleviating the seasonal drought and desiccation of the soils in southern China.

Conclusions

The characteristics of soil aggregates, water infiltration, runoff, sediment, and associated nutrient transport for RCS and BSS at various W-OH concentrations were studied in an indoor controlled experiment and an outdoor simulated rainfall experiment. MWD and GMD of the aggregates of the two soils increased, D decreased, and WSA increased as the W-OH concentration increased and were more variable for BSS than for RCS, indicating that W-OH could increase

Table 3 Mean soil-water contents of the four microplots with simulated rainfall on three measuring occasions

Soil type	W-OH concentration (%)	Before simulated rainfall (%)	After simulated rainfall (%)	24 h after simulated rainfall (%)
RCS	0	8.2	13.3	10.6
	5	9.4	13.1	11.1
BSS	0	9.2	10.9	10.5
	5	8.5	11.0	8.9

RCS, red clay soil; *BSS*, *benggang* sandy soil

aggregation and aggregate stability for the two soils and thus decrease the erodibility of the soils and indicating that BSS responded better than RCS. Spraying with W-OH significantly decreased the rate of water infiltration for both soils, and the rate decreased as the W-OH concentration increased, which directly increased runoff during the simulated rainfall. Spraying with W-OH nevertheless significantly decreased the rate of soil loss and effectively prevented and controlled the erosion of both soils. W-OH also affected the nutrient contents of the runoffs to some extent, strongly affecting TOC content, weakly affecting nitrogen content, and not affecting TK content. The mean SWCs first increased and then decreased before, immediately after, and 24 h after the simulated rainfall, but the difference between 0 and 5% W-OH was not significant, indicating that spraying W-OH did not strongly affect the mean SWC of the aboveground microplots containing 50 cm of soil. The results of this study provide basic data and supplement the theory of applying W-OH in preventing and controlling soil erosion in southern China.

Funding This work was supported by the National Natural Science Foundation of China (41807019), the Natural Science Foundation of Jiangsu Province (BK20181109), the Science and Technology Services (STS) Network Program of the Chinese Academy of Sciences (KFJ-STS-QYZD-093), the National Key Research and Development Program of China (2019YFC1805104), the Jiangsu Provincial Department of Water Resources (2019039), and the Soil and Water Conservation and Ecological Environment Monitoring Station of Jiangsu Province (JSSW201911005).

Compliance with ethical standards

Conflict of interest The authors declare that they have no conflict of interest.

References

Baskan O, Cebel H, Akgul S, Erpul G (2010) Conditional simulation of USLE/RUSLE soil erodibility factor by geostatistics in a Mediterranean Catchment, Turkey. Environ Earth Sci 60:1179–1187

Cao LX, Liang Y, Wang Y, Lu HZ (2015a) Runoff and soil loss from *Pinus massoniana* forest in southern China after simulated rainfall. Catena 129:1–8

Cao LX, Zhang YG, Lu HZ, Yuan JQ, Zhu YY, Liang Y (2015b) Grass hedge effects on controlling soil loss from concentrated flow: a case study in the red soil region of China. Soil Tillage Res 148:97–105

De Baets S, Poesen J, Reubens B, Muys B, De Baerdemaeker J, Meersmans J (2009) Methodological framework to select plant species for controlling rill and gully erosion: application to a Mediterranean ecosystem. Earth Surf Process Landf 34:1374–1392

Deng YS, Shen X, Xia D, Cai CF, Ding SW, Wang TW (2019) Soil erodibility and physicochemical properties of collapsing gully alluvial fans in southern China. Pedosphere 29:102–113

Gao L, Wang YJ, Geris J, Hallett PD, Peng XH (2019) The role of sampling strategy on apparent temporal stability of soil moisture under subtropical hydroclimatic conditions. J Hydrol Hydromech 67:260–270

Gao L, Peng XH, Biswas A (2020) Temporal instability of soil moisture at a hillslope scale under subtropical hydroclimatic conditions. Catena 187:104362

Jia YH, Li TC, Shao MA, Hao JH, Wang YQ, Jia XX, Zheng C, Fu XL, Liu BX, Gan M, Zhao MY, Jv XN (2019) Disentangling the formation and evolvement mechanism of plants-induced dried soil layers on China's Loess Plateau. Agric For Meteorol 269-270:57–70

Jiang FS, Zhan ZZ, Chen JL, Lin JS, Wang MK, Ge HL, Huang YH (2018) Rill erosion processes on a steep colluvial deposit slope under heavy rainfall in flume experiments with artificial rain. Catena 169:46–58

Lal R (2003) Soil erosion and the global carbon budget. Environ Int 29:437–450

Li TC, Jia YH, Shao MA, Shen N (2019) *Camponotus japonicus* burrowing activities exacerbate soil erosion on bare slopes. Geoderma 348:158–167

Liang Y, Ning DH, Li DC, Zhang B (2009) Characteristics and governances of collapsing gully erosion in the red soil region of southern China. Soil and Water Conservation in China 1:31–34

Liang Y, Li DC, Lv XX, Yang X, Pan XZ, Mu H, Shi DM, Zhang B (2010) Soil erosion changes over the past five decades in the red soil region of southern China. J Mt Sci 7:92–99

Liang ZS, Wu ZR, Mohammad N, Yang CQ, Yao WY (2017) A new ecological control method for Pisha sandstone based on hydrophilic polyurethane. J Arid Land 9:790–796

Liang ZS, Wu ZR, Yang CQ, Yao WY, Leng YB (2016) Mechanism of erosion resistance and vegetation promotion by W-OH in Pisha sandstone. J Hydraul Eng 47:1160–1166

Liang ZS, Wu ZR, Yao WY, Noori M, Yang CQ, Xiao PQ, Leng YB, Deng L (2019) Pisha sandstone: causes, processes and erosion options for its control and prospects. Int Soil Water Conserv Res 7:1–8

Lin JS, Huang YH, Wang MK, Jiang FS, Zhang VB, Ge HL (2015) Assessing the sources of sediment transported in gully systems using a fingerprinting approach: an example from South-east China. Catena 129:9–17

Lin JS, Zhu GL, Wei J, Jiang FS, Wang MK, Huang YH (2018) Mulching effects on erosion from steep slopes and sediment particle size distributions of gully colluvial deposits. Catena 160:57–67

Meyer LD, Harmon WC (1979) Multiple intensity rainfall simulator for erosion research on row sideslopes. Trans ASABE 22:100–103

Ministry of water resources (2018) Bulletin of soil and water conservation. Official website of ministry of Water Resources, PRC. http://www.mwr.gov.cn/sj/tjgb/zgstbcgb/201908/t20190820_1353674.html

Ministry of Water Resources, Chinese Academy of Sciences, Chinese Academy of Engineering (2010) Soil erosion prevention and ecological security in China. Science Press, Beijing

Muukkonen P, Hartikainen H, Alakukku L (2009) Effect of soil structure disturbance on erosion and phosphorus losses from Finnish clay soil. Soil Tillage Res 103:84–91

Nimmo JR, Perkins KS (2002) Aggregates stability and size distribution. In: Methods of soil analysis, Part 4-Physical Methods, vol 202. Soil Science Society of America, Inc., Madison, pp 317–328

Qi F, Zhang RH, Liu X, Niu Y, Zhang HD, Li H, Li JZ, Wang BY, Zhang GC (2018) Soil particle size distribution characteristics of different land-use types in the Funiu mountainous region. Soil Tillage Res 184:45–51

Shen H, Zheng F, Wen L, Han Y, Hu W (2016) Impacts of rainfall intensity and slope gradient on rill erosion processes at loessial hillslope. Soil Tillage Res 155:429–436

Sun JW, Zhang GH (2018) Effect of new material W-OH curing agent of soil and water erosion control on the growth of soybean and maize. Journal of Yangtze River Scientific Research Institute 36(37–19):45

Tang SQ, She DL (2018) Synergistic effects of rock fragment cover and polyacrylamide application on erosion of saline-sodic soils. Catena 171:154–165

Tian P, Xu X, Pan C, Hsu K, Yang T (2017) Impacts of rainfall and inflow on rill formation and erosion processes on steep hillslopes. J Hydrol 548:24–39

Wang Y, Fan J, Cao L, Liang Y (2016) Infiltration and runoff generation under various cropping patterns in the red soil region of China. Land Degrad Dev 27:83–91

Yao WY, Wu ZR, Liu H, Xiao PQ, Yang CQ (2015) Experimental research on the anti-erosion and vegetation promotion for sandstone region in the Yellow River basin. Yellow River 37:6–10

Ye L, Tan W, Fang L, Ji L (2019) Spatial analysis of soil aggregate stability in a small catchment of the Loess Plateau, China: II. Spatial prediction. Soil Tillage Res 192:1–11

Zhang ZF, Huang YH, Lin JS, Jiang FS, Zhu GL, Lin ZH, Zeng CB, He KW (2014) Effects of PAM characteristics on runoff and erosion of colluvial deposits in benggang. Research of Soil and Water Conservation 21:1–5

Zhong B, Peng S, Zhang Q, Ma H, Cao S (2013) Using an ecological economics approach to support the restoration of collapsing gullies in southern China. Land Use Policy 32:119–124

Zhu YY, Cao LX, Wu ZR, Chen C, Liang Y (2017) Impact of W-OH on soil detachment rate of colluvial deposits in collapsing hill. Acta Pedol Sin 54:73–80